Microdetection of Chromium Mixed–Valences using CuNiTi Electrode

By Nirwan Syarif

Available free online at www.medjchem.com

Mediterranean Journal of Chemistry **2022**, 12(2), 112-122

Microdetection of Chromium Mixed–Valences using CuNi/Ti Electrode and Linear Sweep Voltammetry

Nirwan Syarif

Departemen of Chemistry, Universitas Sriwijaya, Indralaya, Indonesia 30814

Abstract: An electrode of non-precious metal has the potency to be utilized as a working electrode for voltammetry measurements of Cr^{3+} and Cr^{6+}. The analytical performance of the electrode in determining specific metal species qualitatively and quantitatively was studied. The detection data were recorded and analyzed using cyclic voltammetry (CV) and linear sweep voltammetry (LSV), whereas scanning electron microscope (SEM) and X-ray diffraction (XRD) spectroscopy were used to determine the surface morphology and the presence of crystalline in the electrode. Electroanalytical performance was determined by linear sweep voltammetry. The results show that the reduction of Cr^{6+} to Cr^{3+} appeared at +0.84 V (vs Ag/AgCl) and the reduction of Cr^{3+} to Cr^{2+} at +0.74 V (vs Ag/Ag). The optimum conditions for measuring Cr^{3+} were found at pH 6, deposition time of 30 seconds, and a scan rate of 160 mVs^{-1}. The optimum pH for measuring Cr^{6+} is 4, deposition time of 60 seconds, and a scan rate of 140 mVs^{-1}. The regression curve for the Cr^{3+} is linear in concentration 1 – 10 gL^{-1} with a correlation coefficient of 0.9883 and a detection limit of 2.08 gL^{-1}. While the Cr^{6+} is linear in the range of 1 – 10 gL^{-1} with a correlation coefficient of 0.99 and a detection limit of 2.18 gL^{-1}. There is a slight difference in the individual measurement current and the mixture of Cr^{3+} and Cr^{6+} but with a good agreement for the oxidation-reduction potential. The measurement data analysis shows the feasibility of the electrode and the measurement system developed.

Keywords: alloy; potentiostat; diffractogram; voltammogram; electrolyte.

1. Introduction

One element that is harmful to health is chromium. Chromium is a heavy metal whose presence in the waters. It needs to be analyzed because chromium belongs to hazardous toxic materials. Chromium in water exists in two stable oxidation states, namely Cr^{3+} and Cr^{6+}. Chromium (III) is an important species in living organisms. Chromium (III) plays a role in maintaining the normal glucose, fat, and protein metabolism in mammals [1]. Chromium (VI), inversely, is a toxic and carcinogenic substance to humans, although in relatively low concentrations [2].

Several methods are commonly used for the determination of Cr, such as atomic absorption spectrophotometry (AAS) [3], coupled plasma inductive - atomic emission spectrophotometry (ICP-AES) [4], coupled plasma inductive-mass spectrometry (ICP-MS) [5]. However, these methods require expensive costs and cannot distinguish the Cr species instead of directly measured Cr measuring mixed species. Therefore, the mixed-valence needs to be separated into its valence for the measurement. Several voltammetric methods have been widely used for heavy metal analysis [6]. Voltammetry is an electroanalytical method based on the oxidation-reduction process on the electrode surface. This method allows mixtures of ions to be measured individually in one step [7]. Stripping [8] and cyclic voltammetry [9] were chosen because it has high sensitivity [10], low detection limit on the ppb scale [11], easy use, and easy sample preparation [12].

The electrode is the place for electrochemical processes, i.e., a faradaic process that the electric current generates and a non-faradaic process that ionic absorption takes place at the electrode. The working electrode is where the observed electrochemical reactions occurred. The working electrodes commonly used are metal solids [13] such as gold (Au), platinum (Pt), silver (Ag), semiconductor electrodes [14], and carbon electrodes such as glassy carbon, graphite, or carbon paste [15].

One of the electrodes used is platinum (Pt) electrochemical application. Pt electrodes are known to have the ability to reduce Cr^{6+} to Cr^{3+}. Platinum employs several forms for the analytical application of ionic Cr electrolytes [16]. Electrodeposition for various applications frequently used Pt wire [17], and others such as Pt powder [18], Pt foil [19], and Pt rod for various applications [9]. Pt metal plated on a support metal such as titanium is also worthy of attention because it has an excellent current density [20]. Partial substitution of Pt metal is a frequent step since it is

**Corresponding author: Nirwan Syarif*
Email address: nsyarif@unsri.ac.id

DOI: http://dx.doi.org/10.13171/mjc02208201639syarif

Received June 3, 2022
Accepted July 11, 2022
Published August 20, 2022

relatively costly. Wijenberg et al. reported the ability of Pt/Ir electrodes to carry out oxidation-reduction reactions [21]. The electrode of IrO_2 coated Ti oxidizes simulated wastewater electrochemically [22]. Zn coating on Fe produced by electrodeposition technique [23]. The voltammetry test results from this study indicate the presence of electrochemical activity in the electrolyte solution. Sn coated on the Fe surface was reported to be more likely to have reducing activity. These three reports provide an overview of the feasibility of using electrocatalyst metal alloys with metal supports.

Titanium is a metal widely applied as a support in preparing electrodes [24]. This paper reports the research results on the manufacture of electrodes, namely Cu and Ni metal alloys on the surface of Ti. The measurement conditions, such as pH, deposition time, and scan rate, affect the electrode's linearity and the limit of detection (LOD) [25]. These factors affect the ionic deposition on the electrode's surface and the performance of the measurement.

2. Experimental

2.1. Materials

The electrodes, Ag/AgCl, and Pt were bought from our local company. The chemicals, such as deionized water, Isopropanol (Fluka), and titanium plate, were analytical grade and were used without purification. $NiCl_2$, $6H_2O$, Cu_2O were used as a precursor for preparing electrode. $CrCl_3.6H_2O$ (Merck), $K_2Cr_2O_7$ (Merck), $NaNO_3$ (Merck), EDTA (Merck), and CH_3COONa were used to prepare stock solutions. Sandpaper (Toho) was purchased from the local store.

2.2. Working Electrode

The CuNi/Ti electrode was prepared using $NiCl_2$. $6H_2O$ and Cu_2O as a precursor. Both dissolved in pure isopropanol (Fluka). An electric furnace heated the titanium plate at 400°C to have its rough surface [22]. The titanium plate was sandblasted to ensure good adhesion of the deposit on its surface. After heating, the plate was cleaned using water, rinsed in detergent, and washed in water and isopropanol. This step cleaned the Ti surface from residual sands from sandpaper. The surface dried in an oven at 80°C. The coating was prepared on a rough metal surface. The precursor was coated to the surface using a doctor blade knife on a cleaned and coarse 20 mm x 10 mm titanium (Ti) plate. The coated surface was put in an oven for 15 min at 80°C to allow the solvent is evaporated. Next, the layer was fired at 400°C in the furnace for 15 min to allow the decomposition of the precursor. The procedures were repeated five times to achieve the desired weight of the coating. A 2.5 g of the total mass of the metal alloy used was calculated from its precursor with Cu:Ni (3:1) ratio.

2.3. Measurement setup

Two electrolyte solutions were prepared, i.e., electrolyte content Cr^{3+} and Cr^{6+}. The mixed-valence electrolyte was made from the mixture of Cr^{3+} and Cr^{6+} dissolved in one solution. 0.514 grams of $CrCl_3.6H_2O$ was weighed and dissolved in 100 mL of deionized water. Standard solution of Cr^{3+} ion was prepared from 1000 ppm solution, which was then diluted gradually into several concentrations, namely 0.1; 0.5; 1; 5, and 10 gL^{-1} as much as 100 mL each. Cr^{6+} was made from $K_2Cr_2O_7$ (Merck). $K_2Cr_2O_7$ powder weighed as much as 0.565 grams, then dissolved with distilled water in a 100 mL volumetric flask to the limit mark and stirred to 1000 ppm of Cr^{6+} solution. The standard metal ion Cr^{6+} was prepared from 1000 ppm solution, diluted gradually into several concentrations, i.e., 0.1; 0.5; 1; 5, and 10 gL^{-1} as much as 100 mL each. The electrolyte solution was prepared by mixing 21.3 g $NaNO_3$, 4.46 g EDTA, and 1.64 g NaAc, then dissolved with deionized water in a 100 mL volumetric flask to the mark.

The instrumentation configuration for determining the optimum conditions for measuring Cr^{3+} and Cr^{6+}, as well as for the speciation of Cr^{3+} and Cr^{6+}, is as follows: the PGSTAT204 Autolab Metrohm potentiostat is connected to the electrodes. The other end of the potentiostat was connected to the computer to obtain data and power source. The solution was placed in the potentiostat for cyclic voltammetry and linear sweep voltammetry tests with 3 electrodes in half cell system. The CuNi/Ti was used as the working electrode, Ag/AgCl as the reference electrode, and Pt as the counter electrode in an electrolyte solution containing Cr^{3+} and Cr^{6+}.

2.4. Determination of optimum pH

A 10 ml of 1 gL^{-1} Cr^{3+} solution with 2.5 mL of the electrolyte solution was put into a voltammetry cell with a pH variation of 4,5,6,7 and 8, then measured the current at a potential of -700 mV to 990 mV; deposition time was 30 seconds and scanned 160 mVs^{-1}. Measurement of Cr^{6+} was carried out at a potential window of -700 mV to 990 mV, deposition time of 60 seconds, and a scan rate of 140 mVs^{-1}.

2.5. Determination of deposition time

A 10 mL of 1 gL^{-1} Cr^{3+} solution with 2.5 mL of the electrolyte solution was put into a voltammetry cell at the best pH conditions and then measured with a current at a potential window of -700 mV to 990 mV with variations in deposition time of 0, 15, 30, 60 and 120 seconds, and at a scan rate 160 mVs^{-1}. The measurement of Cr^{6+} was carried out at a potential window of -700 mV to 990 mV and a scan rate of 140 mVs^{-1}.

2.6. Determination of the Optimum Scan Rate

A 10 mL of 1 gL^{-1} Cr^{3+} solution with 2.5 mL of the electrolyte solution was put into a voltammetry cell at the best pH and deposition time and then measured the current at a potential window of -700 mV to 990 mV, with the variations in the scan rate 100, 110, 120, 140, 160, 180, 200 mVs^{-1}. Then, measurement of Cr^{6+} was carried out in the same way as the above procedure.

2.7. Linear Regression Plot

Determination of the regression plot were done by varying the concentration of Cr^{3+} or Cr^{6+} 0.1; 0.5; 1; 5; 10 gL^{-1}. Measurements were carried out at optimum measurement conditions. The concentration of Cr^{6+} solution was prepared using the same procedure.

2.8. Determination of the Limit of Detection

The procedure was done by measuring the concentration of Cr^{3+} and Cr^{6+}, which gives a linear regression of the current. The current response measurement was repeated three times. The limit of detection was obtained from the following calculation using:

$$Sy/_{x} = \frac{\sqrt{(\Sigma(y-\hat{y})^2}}{n-2} \qquad (1)$$

$$LOD = \frac{3\ Sy/x}{a} \qquad (2)$$

Where $S_{y/x}$ is the measurement standard deviation, y is current, n is the number of data, a is the slope of the linear regression curve, and LOD is the detection limit.

3. Results and Discussion

X-ray diffraction measurements were carried out to determine the metal elements composed in the electrode. The diffractogram of the electrode [26] in Figure 1(a) shows the presence of TiNi (2Θ = 26.6, 40.0, 48.8, 54.5) as described in paper [27], and overlaps with the diffraction peak of TiCu (2Θ = 18.15, 40.0, 54.5) refer to the report by reference [28] These elements form alloys and composites of the electrode. These results indicate that the electrode is made of metal, not its oxide. SEM image (Figure 1(a)) confirms the diffractogram. Figure 1(b) shows the SEM representation of the prepared TiNi electrode morphology. The TiCu surface shows overlapping layers of TiNi, cracks, and flakes. The thermal shock that arose during the electrode removal from the oven caused the various cracks observed on the surface of the electrodes. The cracks appeared during their removal from the oven. Ti which Cu well covered, only appeared as low-intensity peaks at 2Θ = 40 and 45, which confirmed the presence of TiCu.

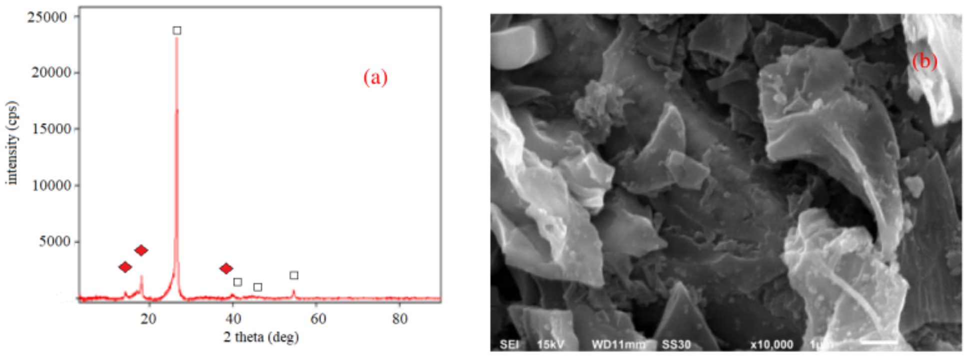

Figure 1. (a) Diffractogram (b) SEM image of the electrode for TiCu and TiNi

The surface of the electrode consists of the main morphology and crack of various sizes. The cracks are impurities cleaned by soaking the electrodes in acetone, washing with detergent, and polished. These flakes reduce the electrical conductivity of the electrolyte solution and the electrodes. As a result, the surface of the main structure of the electrode looks relatively smooth without showing any pores.

Metals for electrodes are generally made of noble metals, such as gold (Au) and platinum (Pt). These metals are relatively more resistant to oxidation. In noble metals, the oxides are found as a black crust on the metal surface following the oxidation occurs. This crust is easy to clean by sweeping it with a cloth. The oxygen comes from metal oxides which is included via oxidation or functional groups of organic molecules. If the chemical bonding is weaker than the physical bonding, the oxides accumulated on the metal surface can be removed from the surface. This situation occurs in precious metals. Resistance to oxidation reactions affects the performance and stability of the electrode.

Preliminary tests were conducted to determine the electrochemical properties of the electrode in reducing Cr^{3+} and Cr^{6+}. The electric current shows this ability as an electrode response to the applied voltage. The tests were done in electrolyte solutions containing Cr^{3+} and Cr^{6+} ions. In addition, cyclic voltammetry measurements are used to provide information about the electrochemical oxidation-reduction reactions that occur in the reaction system and the reversibility of the reactions [29].

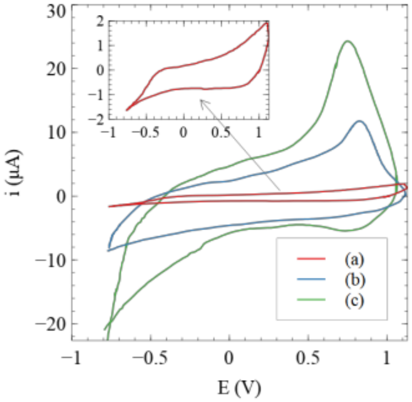

Figure 2. Voltammogram of solution without electrolyte ion (red line), electrolyte solution with 1 gL^{-1} Cr^{3+} (blue line) and (c) electrolyte solution 1 gL^{-1} Cr^{6+}

It can be seen in Figure 2 that the voltammogram of the electrolyte without Cr^{3+} and Cr^{6+} did not show peaks (red line). The peaks are visible in two other voltammograms, revealing the solution's response containing Cr^{3+} and Cr^{6+} (blue and green lines). The peak on the voltammograms for measuring electrolytes concentration of Cr^{3+} and Cr^{6+} ions is in the anodic current. To generate an anodic current, the scan potential runs from low to high values. The opposite direction, cathodic current, shows no peak as expected. It indicates that only reduction reactions occur in electrochemical systems using electrolytes of Cr^{3+} or Cr^{6+} and the electrodes. The faradaic process for reducing ions on the surface of the electrode in response to a given potential is specific.

The electro-reduction of Cr^{6+} to Cr^{3+} occurs at a potential of +1.33 V vs. Standard Hydrogen Electrode (SHE). The potential reduction of Cr^{3+} to Cr^{2+} occurs at -0[illegible] V. In another study, the reduction of Cr^{6+} to Cr^{3+} at a potential of -0.62 V (vs. Ag/A[illegible] [30]. The reduction of Cr^{3+} to Cr^{2+} was found at -0.74 V (vs Ag/AgCl) [31]. The preliminary study of the Cr^{6+} reduction current appeared at +0.84 V (vs. Ag) and Cr^{3+} reduction at +0.74 V (vs. Ag) (Figure 1). The reduction peak shifts from its standard potential are affected by many factors, including the use of electrodes, electrolytes, and measurement conditions [32]. The potentials for the electrochemical reactions in which are implicated various Cr(VI) species were proposed by the other [33] as the probable mechanism. The mechanism for concentrations ≥ 25 mM *K₂CrO₄* is given by the following:

$$HCr_2O_4 + H^+ + 3e^- \Longleftrightarrow (CrO_3^{3-})_{ads} + H_2O$$

$$(CrO_3^{3-})_{ads} + 3HCrO_4^- + H^+ \rightarrow 2(HCr_2O_7)_{ads} + H_2O + 3e^-$$

$$2(HCr_2O_7)_{ads} + 26H^+ + 12e^- \rightleftarrows 4Cr^{3+} + 14H_2O$$

The HCr_2O_7 species adsorbed on the metal surface by the proposed mechanism is

$$M(s) + HCr_2O_7 \overset{-e^-}{\Longleftrightarrow} M^I - HCr_2\,O_7$$

$$M(s) + HCr_2O_7^- \overset{-e^-}{\Longleftrightarrow} M^I - HCr_2\,O_7$$

The reaction competes with the hydroxyl species of water

$$M(s) + HO^- \xrightarrow{-e^-} M^I(OH)$$

$$M(s) + 2H_2O \longrightarrow M^I(OH_2)^{2+}$$

$$M^I(OH_2)^{2+} + HO^- \longrightarrow M^I(OH) \text{ Where M = Cu, Ni}$$

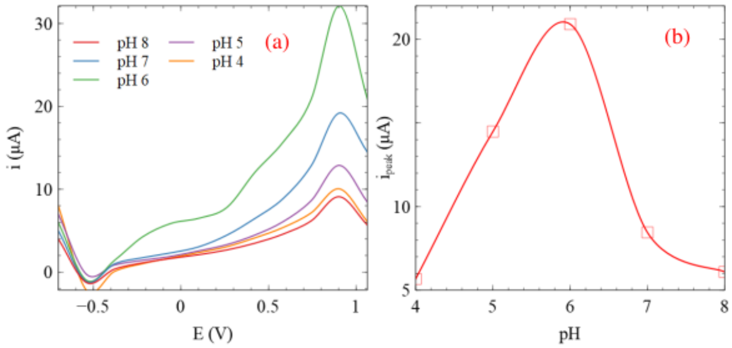

Figure 3. (a) Voltammogram of 1 gL^{-1} Cr^{3+} in pH varies (b) plot of the relationship of the pH Cr^{3+} solution and the current peak of the voltammogram

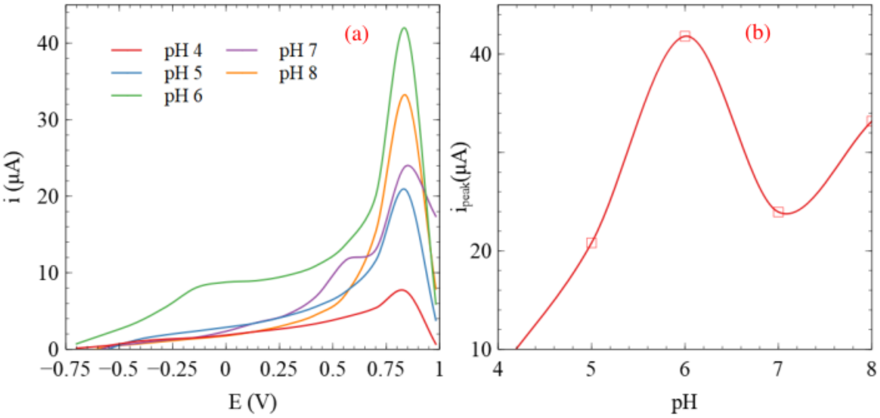

Figure 4. (a) Voltammogram of 1 gL^{-1} Cr^{6+} varied in pH, (b) plot of the relationship of the pH Cr^{6+} solution and the current peak of the voltammogram

3.1. The Conditions for the measurement

The sensitivity of the measurements is affected by the measurement conditions, i.e., pH, deposition time, and the scan rate. For example, scan rate and pH gave linear voltammetry measurements of peak currents as reported by Latif et al. [34] Deposition time affects the ionic deposition on the electrode surface [35]. In general, voltammetry measurements require that the measured faradaic current be slightly larger than the portion of its response to a given potential difference. This condition results in better sensitivity and smaller detection limits.

3.2. Optimum pH

Interaction between electrolyte and electrode takes place on the surface [36] pH affects the electrode surface at metal electrodes, which causes the formation of charged ions on the surface, significantly the negative charge of the water molecule. Therefore, it affects the process at electrode [37].

The effect of pH was studied in pH 4 – 8 by comparing the voltammogram of the solutions containing Cr^{3+} and Cr^{6+}. It is expected that more ions are adsorbed at the surface of the electrode to produce a maximum and stable peak current for the measurement at suitable pH conditions [38].

Figure 3 shows the change in the response of the Cr^{3+} ion. The change in current is proportional to the applied potential. It was found that the maximum pH is 6. Figure 4 shows the change in the response of the Cr^{6+} ion. The change in current is proportional to the applied potential. It was found that the maximum pH is 4. The chromium ion exists in a mixed-valent state [39] with an electric charge depending on the system's pH [40]. When the pH of the solution is between 1 and 6, chromium is in equilibrium as it forms HCrO^{4-} and $Cr_2O_7^{2-}$ When the solution is at 6, Cr^{6+} is in the form of CrO_4^{2-} ions, while the pH is less than 1, the main species is H_2CrO_4. pH 4 was used as the optimum pH for the measurement of Cr^{6+} because the measurement at pH 4 was more stable than another pH, and the measurement at pH 4 could obtain a higher measurement concentration [41].

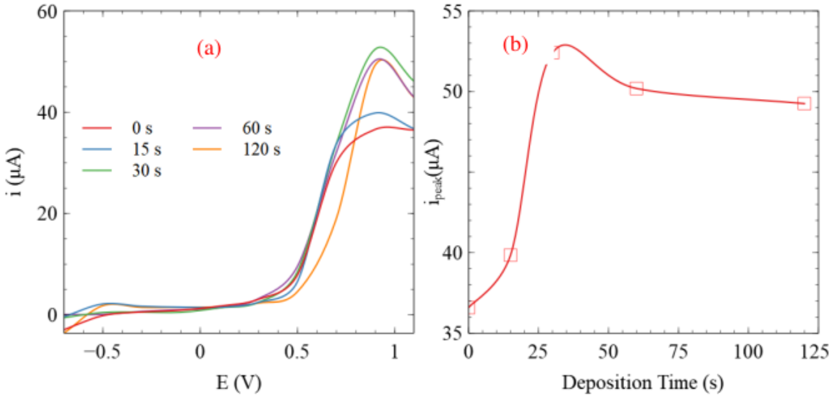

Figure 5. (a) Voltammogram of 1 gL^{-1} Cr^{3+} varies in deposition times. (b) plot relationship of deposition time and current peak of the voltammogram

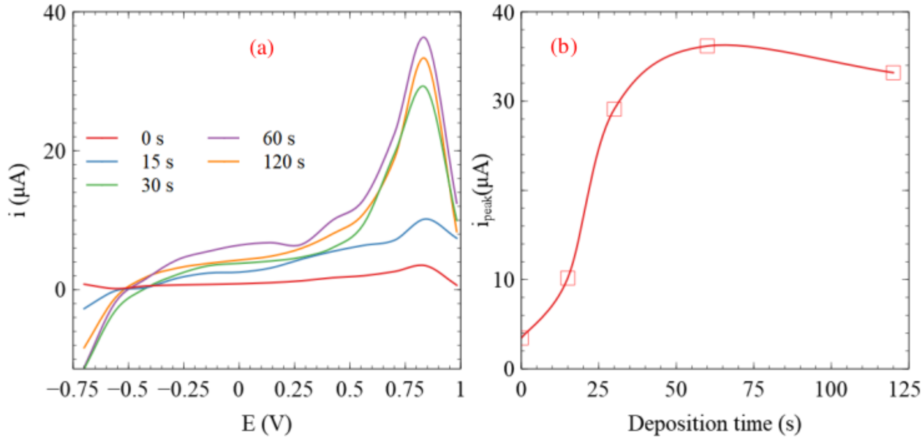

Figure 6. (a) Voltammogram of 1 gL^{-1} Cr^{6+} varies in deposition times, (b) plot relationship of deposition time and current peak of the voltammogram

3.3. Optimum Scan Rate

The scan rate affects the current peak and width of the voltammogram. The Faraday process, i.e., electrochemical oxidation-reduction reaction, causes a current peak. The change in the width of the voltammogram is due to the diffusion of ions to the electrolyte surface. The effect of scan rate was studied by comparing the voltammogram of the measurement results of Cr^{3+} and Cr^{6+} ions at pH conditions and deposition time. The scan rate varied between 100-200 mVs^{-1}. It can be seen from Figures 7 (a) and 8 (a) that the scan rate affects the current peak of Cr^{3+} and Cr^{6+} ions. The current was proportional to the electrochemical reaction rate at the electrode surface. The higher the scan rate, the faster the electrolysis reaction speed so that the peak current increases [42]. The measurement of Cr^{3+} at 160 mVs^{-1} gives the maximum current peak (Figure 7 (a)). The optimum conditions for measuring Cr^{3+} were found at pH 6, deposition time of 30 seconds, and a scan rate of 160 mVs^{-1}. The curve is relatively broader compared to the other scan rate. A widening curve interferes with the measurement, especially if there is interference from other ions with adjacent half-wave potentials, which can cause the curves to overlap. There is a decrease in current peak at a higher scan rate (Figure 7(b) because the metal attached to the electrode surface is saturated, so the Cr^{3+} ions adsorbed on the electrode surface are desorbed. The highest current for the scan rate of Cr^{6+} measurement was 140 mVs^{-1} (Figure 8 (a)). The optimum pH for measuring Cr^{6+} is 4, deposition time of 60 seconds, and a scan rate of 140 mVs^{-1}. Two maxima exist in the measurement involving the relationship between the scan rate and the current peak.

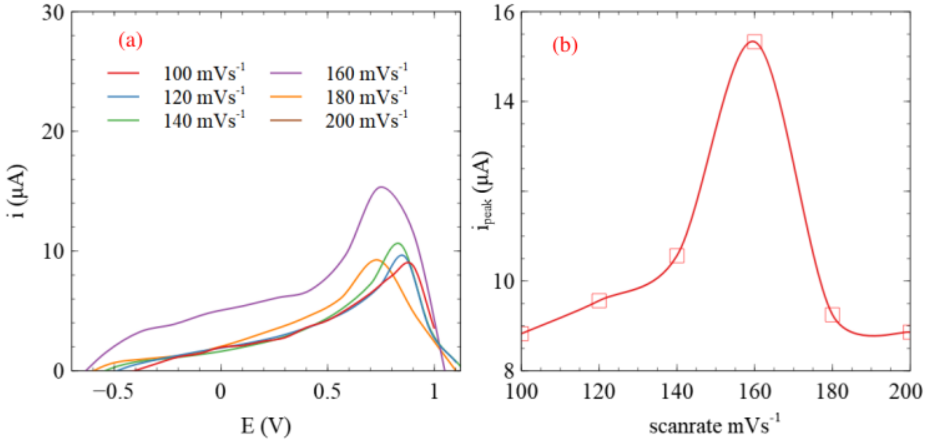

Figure 7. (a) Voltammogram of 1 gL^{-1} Cr^{3+} in various scan rates (b) Plot of the relationship between scan rate and current peak of the measurement

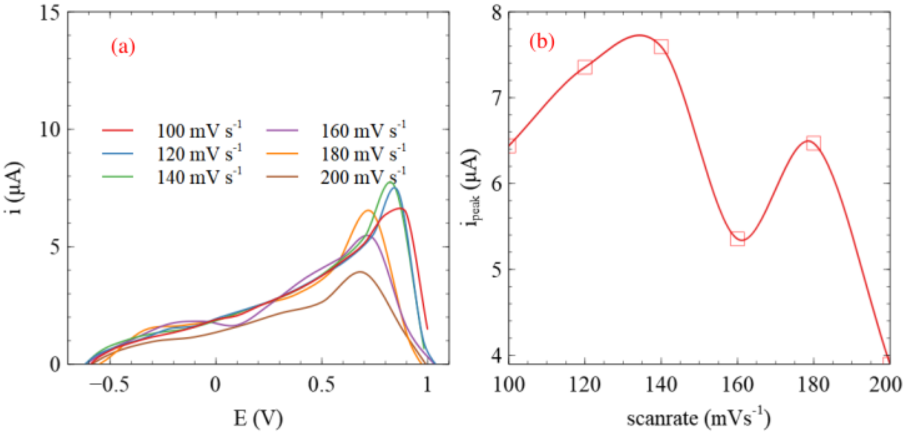

Figure 8. (a) Voltammogram of 1 gL^{-1} Cr^{6+} in various scan rates. (b) Plot of the relationship between scan rate and the current peak of the measurement

3.4. Linear Regression of Cr^{3+} and Cr^{6+} Voltammograms

A measurement contains linear and nonlinear parts in a certain measurement range. The linear portion of the measurement is used to quantify the linearity of the measurement. This method is applied to obtain the linearity of Cr^{3+} and Cr^{6+} measurements using voltammetry cyclic and the electrode. The linear regression plot was formed from the LSV measurement data for each type of ion. Each type of ion measured varied its concentration in the electrolyte solution, i.e., 0.1; 0.5; 1; 5 and 10 gL^{-1}. The measurements were carried out at pH, deposition, and scan rate to reach maximum current (ip) conditions in anodic current.

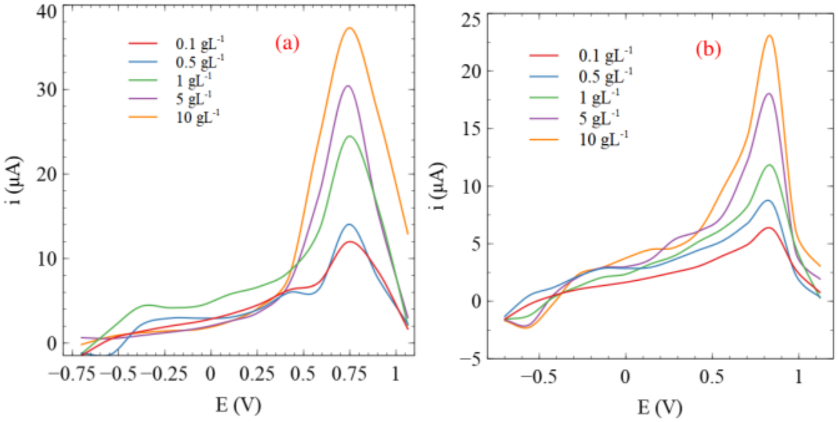

Figure 9. Voltammograms of (a) Cr^{3+} and (b) Cr^{6+} measurements using each optimal condition

The voltammograms for each measurement of Cr^{3+} and Cr^{6+} and their concentration variations are shown in Figure 9. The maximum currents or current peaks (i_p) in Figure 9 were plotted for a regression plot. The regression plot of the Cr^{3+} and Cr^{6+} standard solution is presented in Figures 10 and 11.

Figure 10 (a) shows the current peak (ip) obtained at a concentration of 0.1-0.5 gL^{-1} from Figure 10 (a) as the base to determine the linearity of measurement. Statistical calculations of the plot give 0.8248 for the correlation coefficient (r) and $y = 2.3435x + 16.037$ for the plot equation. The value of r provides information for the fitness of experimental data and the plot of mathematical equations [43].

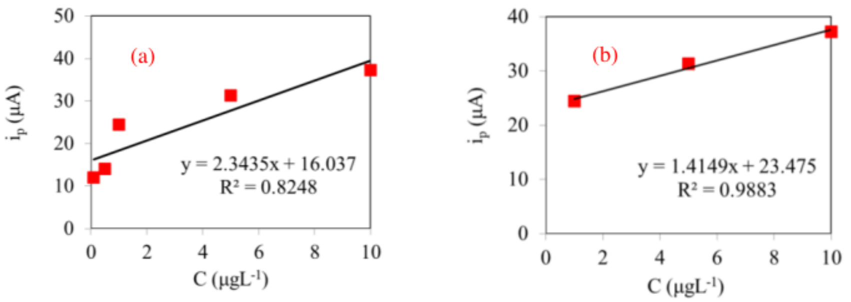

Figure 10. (a) regression plot for i_p versus C of Cr^{3+} ion, (b) linear part of regression plot for Cr^{3+}

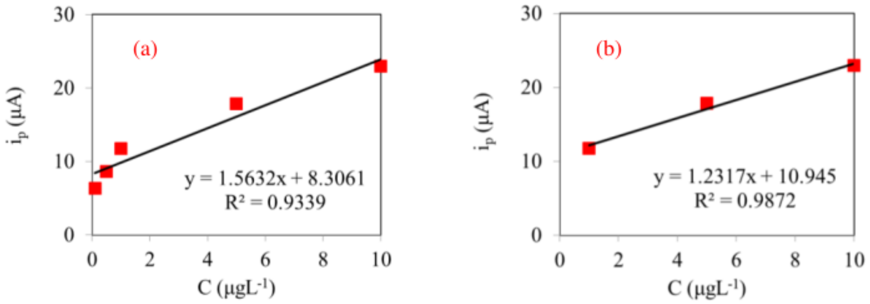

Figure 11. (a) Regression plot for i_p versus C of Cr^{6+} ion, (b) linear part of regression plot for Cr^{6+}

Some points from the measurement need to be removed to increase the measurement's fitness. The last two points, namely C= 0.1 and 0.5, were removed from the regression pl[illegible]o that a new regression line was obtained with the value of the correlation coefficient (r) = [illegible]9883 and y = 1.415 x + 23.475 (Figure 9(b)). It can be seen from Figure 10 (b) that the current increases with increasing Cr^{3+} concentration. Due to the increasing concentration of Cr^{3+}, the greater the amount of Cr^{3+} in the solution reduced Cr^{2+} on the electrode surface.

Figure 11 (a) shows the plot of the current peak versus the concentration of the voltammogram in Figure 9 (b). Regression plot has equation y = 1.5623 x + 8.3061 and correlation coefficient (r) is 0.9339. The value is considered to be less linear. The same steps were also taken to produce a more fit plot. Two first points were removed from the measurement. It can be shown from Figure 11 (b) that the plot has equation y = 1.2317 x + 10.945 with the correlation coefficient (r) = 0.9872.

[illegible] Detection Limit of Measurements

The limit of detection (LOD) determines the lowest concentration detected. The LODs were calculated from the linear regression plot (Figure 10 (b) and 11(b)) using equations (1) and (2) [44]. The measurements were carried out at the optimum pH. The LOD value for Cr^{3+} and Cr^{6+} are 2.082 and 2.182 gL^{-1}, respectively. These values indicate that the accurate measurement for Cr^{3+} and Cr^{6+} can be obtained from the concentration above those concentrations.

3.6. Detection of Cr^{3+} and Cr^{6+} in the Mixture

The mixed-valence electrolyte was prepared from the individual electrolyte solution of Cr^{3+} and Cr^{6+}. The current peaks of the mixture (Figure 12a) show different profiles from the others produced by individual measurements of Cr^{3+}. Voltammograms of the mixed-valence electrolyte of Cr^{3+} and Cr^{6+} for 1 and 10 µgL^{-1} are shown in Figure 12b. The Cr^{6+} has a more negative potential than Cr^{3+} due to its standard potential [45] and is more mobile in an aqueous solution [46].

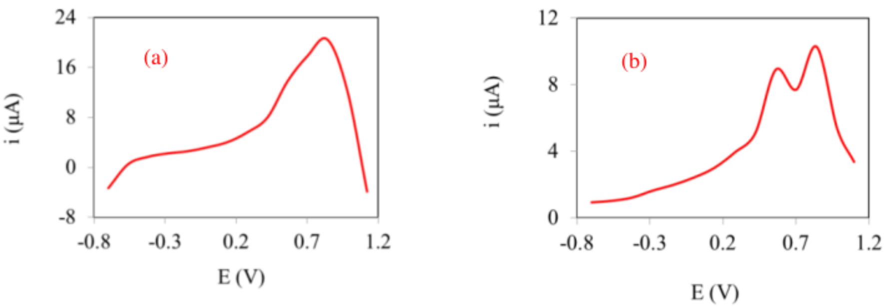

Figure 12. Voltammogram of Cr^{3+} and the mixed electrolyte with concentration (a) 1 μgL^{-1} (b) 10 μgL^{-1}

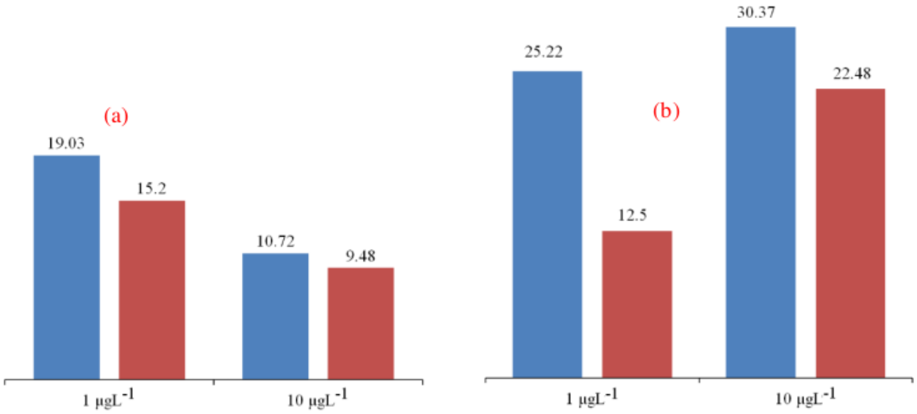

Figure 13. The current peaks of Cr^{3+}■ and Cr^{6+}■ in (a) mixture (b) individually electrolyte solution

The i with a more negative reduction potential tend to be deposited on the electrode surface with a m positive reduction potential. Cr^{3+} was reduced first on the electrode surface, followed by a reduction of Cr^{6+}. The more concentration of Cr^{6+} in the m ure then deposited on the surface of Cr^{3+} is directly proportional to the current peak of Cr^{3+}. The current of Cr^{6+} in the mixture decreased due to the presence of the ion, which was deposited on t surface of Cr^{3+}. The Cr^{6+} was reduced to Cr^{3+} in the reduction potential.

The peak current of the mixture (Figure 13a) compared to the individual measurement results described in Figure 8. Plots in Figure 13b reveal that the results of individual measurements at 10 gL^{-1} are slightly different from those of electrolytes in the mixture. The current peak for the Cr^{6+} ion is not visible at a concentration of 1 gL^{-1}. Instead, the peak current is detected as a slight indentation that slightly changes the slope of the voltammogram. These results indicate that both sparks plug electrodes and voltammetry methods can be used to detect the presence of Cr^{3+} and Cr^{6+} in the solution, which means it is detected not as total Cr but as its ionic valences.

4. Conclusions

X-ray diffraction measurements were carried out to determine the metal elements composed in the electrode. The diffractogram of the electrode shows the presence of TiNi (2ϴ = 26.6, 40.0, 48.8, 54.5) and overlaps with the diffraction peak of TiCu (2ϴ = 18.15, 40.0, 54.5). The surface consists of the main structure of e electrode and crack of various sizes. Preliminary tests were conducted to determine the electrochemical properties of the electrode in reducing Cr^{3+} and Cr^{6+}. The electric current shows this ability as an electrode response to the applied voltage. The tests were done in electrolyte solutions containing Cr^{3+} and Cr^{6+} ions. Cyclic voltammetry measurements are used to provide information about the electrochemical oxidation-reduction reactions that occur in the reaction system and the reversibility of the reactions. The reduction of Cr^{6+} to Cr^{3+} appeared at +0.84 V (vs Ag/AgCl) and the reduction of Cr^{3+} to Cr^{0} at +0.74 V (vs Ag/Ag). The optimum conditions for measuring Cr^{3+} were found at pH 6, deposition time 30 seconds, and scan rate 160 mVs^{-1}, while for measuring Cr^{6+} at pH 4, deposition time 60 seconds, and scan rate 140 mVs^{-1}. The accurate measurement for Cr^{3+} and Cr^{6+} can be obtained from LOD value which are The LOD value for Cr^{3+} and Cr^{6+} are 2.082 and 2.182 gL^{-1}. There is a slight difference in the individual measurement current and the mixture of Cr^{3+} - Cr^{6+} but a good agreement for the oxidation-reduction potential. These results indicate that the electrode and voltammetry methods can be used to detect the presence of Cr^{3+} and Cr^{6+} in the sample separately, which means it is detected not as total Cr but as its species. The data analysis shows the electrode's feasibility considering this measurement system's ability to provide a good current response when applying to the ppb range.

Acknowledgements

The research/publication of this article was funded by DIPA of the Public Service Agency of Universitas Sriwijaya 2021. SP DIPA-042.01.2.400935/2019, On December 05, 2018. In accordance with the Rector's Decree Number: 0145/UN9/SB3.LP2M.PT/2019.

References

1- A. Chait, L. J. den Hartigh, Adipose Tissue Distribution, Inflammation and Its Metabolic Consequences, Including Diabetes and Cardiovascular Disease, Front. Cardiovasc. Med., **2020**, 7, 22.
2- E. Sawicka, K. Jurkowska, A. Piwowar, Chromium (III) and chromium (VI) as important players in the induction of genotoxicity–current view, Ann. Agric. Environ. Med., **2021**, 28, 1.
3- A. M. de O. Lopes, P. R. Chellini, R. A. de Sousa, Cadmium and Chromium Determination in Herbal Tinctures Employing Direct Analysis by Graphite Furnace Atomic Absorption Spectrometry (GF-AAS), Anal. Lett., **2020**, 53, 2096-2110.
4- E. Tsanaktsidou, G. Zachariadis, Titanium and Chromium Determination in Feedstuffs Using ICP-AES Technique, Separations, **2019**, 7, 1.
5- J. B. Vera, M. C. Bisinoti, C. D. B. Amaral, M. H. Gonzalez, ICP- quadrupole MS for accurate determination of chromium in environmental and food matrices, Environ. Nanotechnol. Monit. Manag., **2021**, 15, 100421.
6- A. Ait sidi mou, A. Ouarzane, M. El Rhazi, Detection of mercury by a new sensor-based CPE modified with extract of takaout plant, Mediterr. J. Chem., **2016**, 5, 514–520.
7- N. M. Thanh, N. D. Luyen, T. Thanh Tam Toan, N. Hai Phong, N. Van Hop, Voltammetry Determination of Pb(II), Cd(II), and Zn(II) at Bismuth Film Electrode Combined with 8-Hydroxyquinoline as a Complexing Agent, J. Anal. Methods. Chem., **2019**, 2019, 1.
8- J. Barón-Jaimez, M. R. Joya, J. Barba-Ortega, Anodic stripping voltammetry–ASV for determination of heavy metals, J. Phys. Conf. Ser., **2013**, 466, 012023.
9- S. T. Palisoc, R. I. M. Vitto, M. G. Noel, K. T. Palisoc, M. T. Natividad, Highly sensitive determination of heavy metals in water prior to and after remediation using Citrofortunella Microcarpa, Sci. Rep., **2021**, 11, 1-14.
10- Y. Liu, J. Liu, J. Liu, W. Gan, B. Ye, Y. Li, Highly sensitive and selective voltammetric determination of dopamine using a gold electrode modified with a molecularly imprinted polymeric film immobilized on flaked hollow nickel nanospheres, Microchim. Acta, **2017**, 184, 1285-1294.
11- J. Lalmalsawmi, Zirlianngura, D. Tiwari, S. M. Lee, Low cost, highly sensitive and selective electrochemical detection of arsenic (III) using silane grafted based nanocomposite, Environ. Eng. Res., **2019**, 25, 579.
12- H. Suyani, I. Rahmi, H. Pardi, Optimization for the Simultaneous Determination of Zinc in Environmental Samples With Calcon by Adsorptive Stripping Voltammetry : Response Surface Methodology, Orient. J. Chem., **2017**, 33, 2060.
13- C. M. Welch, R. G. Compton, The use of nanoparticles in electroanalysis: a review, Anal. Bioanal. Chem., **2006**, 384, 601-619.
14- Y. B. Vogel, J. J. Gooding, S. Ciampi, Light-addressable electrochemistry at semiconductor electrodes: redox imaging, mask-free lithography and spatially resolved chemical and biological sensing, Chem. Soc. Rev., **2019**, 48, 3723-3739.
15- D. M. Heard, A. J. J. Lennox, Electrode Materials in Modern Organic Electrochemistry, Angew. Chem., **2020**, 132, 18866-18884.
16- G. E. Badea, C. Antal, M. Rosca, A. Setel, Autocatalytic Reduction of Cr(VI) on Platinum Electrode in Acid Solution, Rev. Roum. Chim., **2012**, 57, 29–33.
17- W. Liu, G. Liu, S. Xiao, J. Zhang, The Electrochemical Behavior of Cr(II) Ions in NaCl-KCl Melt, *Int. J.* Electrochem. Sci., **2017**, 1589-1599.
18- L. Dunyushkina, A. Pavlovich, A. Khaliullina, Activation of Porous Pt Electrodes Deposited on YSZ Electrolyte by Nitric Acid Treatment, Materials, **2021**, 14, 5463.
19- M. A. Ehsan, M. H. Suliman, A. Rehman, A. S. Hakeem, A. Al Ghanim, M. Qamar, Fabrication of platinum thin films for ultra-high electrocatalytic hydrogen evolution reaction, Int. J. Hydrog. Energy., **2020**, 45, 15076-15085.
20- W. Wu, Z. Chen, B. Li, X. Cong, Q. Chen, Mechanical and electrochemical properties of platinum coating by double glow plasma on titanium alloy substrate, Russ. J. Electrochem., **2013**, 49, 76–80.
21- J. H. O. J. Wijenberg, A. C. A. de Vooys, R. Kortlever, M. T. M. Koper, Oxidation reactions in chromium(III) formate electrolytes at platinum and at a catalytic mixed metal oxide coating of iridium oxide and tantalum oxide, Electrochimica Acta, **2016**, 213, 194–200.
22- T. A. F. Appia, L. Ouattara, Electrooxidation of simulated wastewater containing pharmaceutical amoxicillin on thermally prepared IrO_2/Ti, Mediterr. J. Chem., **2021**, 11, 172-184.
23- M. Ouakki, A. El Fazazi, M. Cherkaoui, Electrochemical deposition of Zinc on mild steel, Mediterr. J. Chem., **2019**, 8, 30–41.
24- A. R. Baqer, A. A. Beddai, M. M. Farhan,

B. A. Badday, M. K. Mejbel, Efficient coating of titanium composite electrodes with various metal oxides for electrochemical removal of ammonia, Results Eng., **2021**, 9, 100199.

25- H. H. Hasan, I. H. A. Badr, H. T. M. Abdel-Fatah, E. M. S. Elfeky, A. M. Abdel-Aziz, Low cost chemical oxygen demand sensor based on electrodeposited nano-copper film, Arab. J. Chem., **2018**, 112, 172-180.

26- A. A. Korda, S. Munawaroh, E. A. Basuki, The Antimicrobial Activity and Characterization of the Cast Titanium Copper Alloys with Variations of Copper Content, IOP Conf. Ser. Mater. Sci. Eng., **2019**, 547, 012002.

27- G. Wilhelm Sievers, K. Anklam, R. Henkel, T. Hickmann, V. Brüser, Corrosion-protection of moulded graphite conductive plastic bipolar plates in PEM electrolysis by plasma processing, Int. J. Hydrog. Energy, **2019**, 44, 2435–2445.

28- F. Saba, E. Garmroudi-Nezhad, F. Zhang, L. Wang, Fabrication, mechanical property and *in vitro* bioactivity of hierarchical macro-/micro-/nano-porous titanium and titanium molybdenum alloys, J. Mater. Res., **2020**, 35, 2597–2609.

29- N. Elgrishi, K. J. Rountree, B. D. McCarthy, E. S. Rountree, T. T. Eisenhart, J. L. Dempsey, A Practical Beginner's Guide to Cyclic Voltammetry, J. Chem. Educ., **2018**, 95, 197–206.

30- Q. Ge, X. Feng, R. Wang, R. Zheng, S. Luo, L. Duan, Y. Ji, J. Lin, H. Chen, Mixed Redox-Couple-Involved Chalcopyrite Phase $CuFeS_2$ Quantum Dots for Highly Efficient Cr(VI) Removal, Environ. Sci. Technol., **2020**, 54, 8022-8031.

31- N. Mehdipour, M. Rezaei, Z. Mahidashti, Influence of glycine additive on corrosion and wear performance of electroplated trivalent chromium coating, Int. J. Miner. Metall. Mater., **2020**, 27, 544-554.

32- B. Vercelli, S. Crotti, M. Agostini, Voltammetric responses at modified electrodes and aggregation effects of two anticancer molecules: irinotecan and sunitinib, New J. Chem., **2020**, 44, 18233-18241.

33- S. Trasatti, Work function, electronegativity, and electrochemical behaviour of metals, J. Electroanal. Chem. Interfacial Electrochem., **1972**, 39, 163–184.

34- I. A. Latif, S. H. Merza, Effect of Scan Rate and pH on Determination Amoxilline Using Screen Printed Carbon Electrode Modified with Functionalized Graphene Oxide, Ibn Al-Haitham J. Pure Appl. Sci., **2018**, 31, 157–171.

35- A. Bobrowski, A. Królicka, R. Bobrowski, Renewable silver amalgam film electrodes in electrochemical stripping analysis-a review, J. Solid State Electrochem., **2016**, 20, 3217–3228.

36- A. T. Kuhn, C. Y. Chan, pH changes at near-electrode surfaces, J. Appl. Electrochem., **1983**, 13, 189.

37- A. Goyal, M. T. M. Koper, The Interrelated Effect of Cations and Electrolyte pH on the Hydrogen Evolution Reaction on Gold Electrodes in Alkaline Media, Angew. Chem. Int. Ed., **2021**, 60, 13452-13462.

38- A. Ganassin, P. Sebastián, V. Climent, W. Schuhmann, A. S. Bandarenka, J. Feliu, On the pH Dependence of the Potential of Maximum Entropy of Ir(111) Electrodes, Sci. Rep., **2017**, 7, 1-14.

39- X. Guo, A. Liu, J. Lu, X. Niu, M. Jiang, Y. Ma, X. Liu, M. Li, Adsorption Mechanism of Hexavalent Chromium on Biochar: Kinetic, Thermodynamic, and Characterization Studies, ACS Omega, **2020**, 5, 27323-27331.

40- A. G. Caporale, A. Violante, Chemical Processes Affecting the Mobility of Heavy Metals and Metalloids in Soil Environments, Curr. Pollut. Rep., **2016**, 2, 15-27.

41- M. Tumolo, V. Ancona, D. De Paola, D. Losacco, C. Campanale, C. Massarelli, V. F. Uricchio, Chromium Pollution in European Water, Sources, Health Risk, and Remediation Strategies: An Overview, Int. J. Environ. Res. Public Health, **2020**, 17, 5438.

42- A. A. Bojang, H. S. Wu, Characterization of Electrode Performance in Enzymatic Biofuel Cells Using Cyclic Voltammetry and Electrochemical Impedance Spectroscopy, Catalysts, **2020**, 10, 782.

43- D. Chicco, M. J. Warrens, G. Jurman, The coefficient of determination R-squared is more informative than SMAPE, MAE, MAPE, MSE and RMSE in regression analysis evaluation, Peer J. Comput. Sci., **2021**, 7, e623.

44- R. Ismail, H. Y. Lee, N. A. Mahyudin, F. Abu Bakar, Linearity study on detection and quantification limits for the determination of avermectins using linear regression, J. Food Drug Anal., **2014**, 22, 407-412.

45- M. J. Jorge, M. C. Nilson, H. R. Aracely, F. Machuca-Martínez, Data on the removal of metals (Cr, Cr, Cd, Cu, Ni, Zn) from aqueous solution by adsorption using magnetite particles from electrochemical synthesis, Data Brief, **2019**, 24, 103956.

46- R. Heydarzadeh, A. A. Ghadimkhani, A. Torabian, An improvement of Cr^{+6} removal by the reduction to Cr^{+3} in Birjand ground water treatment, Water Pollution VIII: Modelling, Monitoring and Management, **2006**, 1, 195-202.

Microdetection of Chromium Mixed–Valences using CuNiTi Electrode

ORIGINALITY REPORT

10%
SIMILARITY INDEX

PRIMARY SOURCES

1	comengapp.unsri.ac.id Internet	34 words — 1%
2	mdpi-res.com Internet	32 words — 1%
3	Foffié Thiery Auguste Appia, Lemeyonouin Aliou Guillaume Pohan, Mohamed Berté, Lassiné Ouattara. " Electrochemical comparative study of Ti/Ta O /Pt ‐ RuO ‐ IrO and Ti/Ta O /Pt anodes: Stability, service lifetime, and electrooxidation performance ", Asia-Pacific Journal of Chemical Engineering, 2021 Crossref	29 words — 1%
4	archive.org Internet	19 words — < 1%
5	Murat Sari, Tahir Cosgun, Ibrahim Ertugrul Yalcin, Mahmut Taner, Ibrahim Ilker Ozyigit. "Deciding Heavy Metal Levels in Soil Based on Various Ecological Information through Artificial Intelligence Modeling", Applied Artificial Intelligence, 2021 Crossref	18 words — < 1%
6	pubs.rsc.org Internet	18 words — < 1%

7	Qingui Yang, Chun Yang, Jian Yi, Gaochao Fan, Haipeng Yang, Zaochuan Ge. "A Sensitive Carbon Paste Electrode for Selective Detection of Lead Based on the Synergistic Effect of Bismuth and Chelating Agent", ECS Journal of Solid State Science and Technology, 2020 Crossref	17 words — < 1%
8	Kumar, Nitin. "Mechanical and Structural Behavior of Compressed and Stabilized Earth Block Masonry Systems", University of California, Davis, 2023 ProQuest	16 words — < 1%
9	Muhammad Nurdin, Muhammad Zakir Muzakkar, Maulidiyah Maulidiyah, Trisna Trisna et al. "High Performance COD Detection of Organic Compounds Pollutants using Sulfurized-TiO2/Ti Nanotubes Arrays Photoelectrocatalyst", Research Square Platform LLC, 2022 Crossref Posted Content	16 words — < 1%
10	www.researchgate.net Internet	15 words — < 1%
11	scielo.pt Internet	14 words — < 1%
12	revroum.lew.ro Internet	13 words — < 1%
13	Abdelaziz Ait Sidi Mou, E. E. Ghanjaoui, M. Daoudi, B. El Gamany. "Study on qualitative analysis in cosmetic takaout plant by multivariate statistical", International Journal of Advanced Chemistry, 2020 Crossref	12 words — < 1%
14	web.natur.cuni.cz Internet	12 words — < 1%

15	www.ajol.info Internet	12 words — < 1%
16	"Detection of mercury by a new sensor based CPE modified with extract of takaout plant", 'Mediterranean Journal of Chemistry' Internet	11 words — < 1%
17	academic.oup.com Internet	11 words — < 1%
18	assets.researchsquare.com Internet	11 words — < 1%
19	www.sensorsportal.com Internet	10 words — < 1%
20	LinLin Kong, MeiXiu Kan, DongMei Han, Ting Wang, HuiMin Zhang. "Highly sensitive response to dopamine at a modified electrode involving a composite film with Au nanoparticles dispersed in a fluorocarbon polymer", Science China Chemistry, 2010 Crossref	9 words — < 1%
21	Mohamed M. El-Wekil, Ashraf M. Mahmoud, Adel A. Marzouk, Saad A. Alkahtani, Ramadan Ali. "A novel molecularly imprinted sensing platform based on MWCNTs/AuNPs decorated 3D starfish like hollow nickel skeleton as a highly conductive nanocomposite for selective and ultrasensitive analysis of a novel pan-genotypic inhibitor velpatasvir in body fluids", Journal of Molecular Liquids, 2018 Crossref	9 words — < 1%
22	Zeng, K.. "Recent progress in alkaline water electrolysis for hydrogen production and	9 words — < 1%

	applications", Progress in Energy and Combustion Science, 201006 Crossref	
23	eprints.utas.edu.au Internet	9 words — < 1%
24	repositorio.unesp.br Internet	9 words — < 1%
25	resolver.caltech.edu Internet	9 words — < 1%
26	www.chemweb.com Internet	9 words — < 1%
27	www.nature.com Internet	9 words — < 1%
28	Israel Leka Lera, Sutripto Khasnabis, Lodrick Makokha Wangatia, Olu Emmanuel Femi, Praveen C. Ramamurthy. "An innovative catalyst of PdNiP nanosphere deposited PEDOT:PSS/rGO hybrid material as an efficient electrocatalyst for alkaline urea oxidation", Polymer Bulletin, 2022 Crossref	8 words — < 1%
29	Mohammad Ali Sheikh Beig Goharrizi, Reza Kazemi Oskuee, Ghazaleh Aleyaghoob, Taraneh Mohajeri et al. " A new molecularly imprinted polymer electrochemical sensor based on CuCo O /N - doped CNTs/P - doped GO nanocomposite for detection of 25 - hydroxyvitamin D in serum samples ", Biotechnology and Applied Biochemistry, 2022 Crossref	8 words — < 1%
30	Shima Haghighat, Jahan M. Dawlaty. "pH Dependence of the Electron-Transfer Coefficient:	8 words — < 1%

Comparing a Model to Experiment for Hydrogen Evolution Reaction", The Journal of Physical Chemistry C, 2016
Crossref

---

31 d-nb.info
Internet
8 words — < 1%

---

32 etd.uwc.ac.za
Internet
8 words — < 1%

---

33 qspace.library.queensu.ca
Internet
8 words — < 1%

---

34 Ghodbane, O.. "Copper electrodeposition on pyrolytic graphite electrodes: Effect of the copper salt on the electrodeposition process", Electrochimica Acta, 20070525
Crossref
7 words — < 1%

---

35 Shella Permatasari Santoso, Alfin Kurniawan, Artik Elisa Angkawijaya, Hardy Shuwanto et al. "Removal of Heavy Metals from Water by Macro-Mesoporous Calcium Alginate–Exfoliated Clay Composite Sponges", Chemical Engineering Journal, 2022
Crossref
7 words — < 1%

---

36 Afzal Shah. "A Novel Electrochemical Nanosensor for the Simultaneous Sensing of Two Toxic Food Dyes", ACS Omega, 2020
Crossref
6 words — < 1%

---

37 Endale Tesfaye, Bhagwan Singh Chandravanshi, Negussie Negash, Merid Tessema. "A new modified carbon paste electrode using N1-hydroxy-N1,N2-diphenylbenzamidine for the square wave anodic stripping voltammetric determination of Pb(II) in environmental samples", Sensing and Bio-Sensing Research, 2022
Crossref
6 words — < 1%

EXCLUDE QUOTES	OFF	EXCLUDE SOURCES	OFF
EXCLUDE BIBLIOGRAPHY	ON	EXCLUDE MATCHES	OFF